Brain Tumour Diagnostic Support Based on Medical Image Segmentation

Z. Měřínský, E. Hošťálková, A. Procházka

Institute of Chemical Technology, Prague
Department of Computing and Control Engineering

Abstract

High-grade gliomas represent rapidly growing malignant brain tumours. Early diagnostics of this decease and immediately applied treatment entails better life prognosis for the patient. The goal of this work is to initialize the development of an automated tumour recognition method based on computed tomography images processing. The resulting method is aimed at early glioma diagnostics support by distinguishing between the healthy tissue and the tumour tissue. The proposed technique involves, subsequently, image preprocessing, feature extraction, and classification of the extracted features using an artificial neural network. To obtain features, we compute the skewness of the discrete wavelet transform coefficients from selected rectangular image regions using three neighboring image slices to increase the number of samples while preserving good segmentation resolution within the image. The segmentation results are evaluated in cooperation with the neurologist. For all computations and visualizations, we exploit Matlab.

1 Introduction

High-grade gliomas, namely grade III and IV, represent rapidly growing malignant brain tumours. Early diagnostics of this decease and immediately applied treatment entails better life prognosis for the patient. Computed Tomography (CT) is usually the first examination imaging technique used when certain symptoms occur, due to its lower cost in comparison with Magnetic Resonance (MR). The problem is that, in CT scans, early tumour stages are poorly recognizable and, in approximately two-months time, the tumour grows to such a great size that it is too late for effective treatment as shown in Fig. 1.

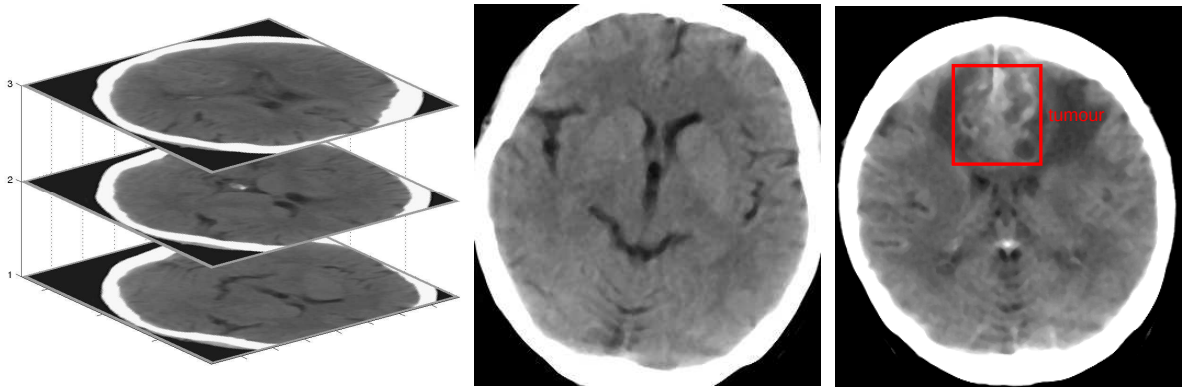

(a) Three CT slices (b) Early stage (c) Later stage

Figure 1: Three consecutive CT image slices **(a)** and selected slices depicting the toumor in an early stage **(b)** and in a later stage after three months with marked tumour area **(c)**

The goal of this work is to initialize the work on an automated CT image segmentation method which should support early glioma diagnostics. The proposed technique involves, subsequently, image preprocessing by median filtering [4], feature extraction [8], and extracted features classification using an artificial neural network [10, 9]. The segmentation results are evaluated

in cooperation with neurologist Dr. O. Vyšata. For all computations and visualizations we use the Matlab environment [5].

2 Features Selection

The process of feature selection is a crucial part of the whole image segmentation task [8]. The choice of feature combination is driven by the features ability to consistently characterize image similar Regions Of Interest (ROI) and distinguish between different regions, which are in our case the healthy and the tumour tissue.

In this paper, the design of the feature computation procedure partially inspired by the recent work [6, 7] by Prof. Petrou from the Imperial College, London. For glioma boundaries detection in MR images of T1 and T2 modalities, Prof. Petrou exploits statistically significant differences between the skewness of the highly-vascular tumour regions and the regions of the surrounding brain tissue. The exact tumour boundary is not recognizable by the eye, same as the changes of the skewness. The skewness is the third order standardized statistical moment and represents the measure of asymmetry of the probability distribution and equals zero for perfectly symmetrical distributions such as the normal distribution. The skewness of a random variable x is defined as

$$\gamma = \frac{E[x-\mu]^3}{\sigma^3} \tag{1}$$

where $E[\,]$ stands for the expected value, μ is the mean of x, and σ is the standard deviation of x, i.e. the first and the second statistical moment, resp.

Since the space-domain-based skewness standing alone is not sufficient for succesful image segmentation, we also employ other features computed by the Discrete Wavelet Transform (DWT) [3] which has been successfully used in many image segmentation applications [2].

The DWT is computed as the convolution of the signal x with a filter bank represented by the lowpass scaling filter h_0 and the highpass wavelet filter h_1. This procedure and the subsequent downsampling by 2 is given as

$$L_1(n) = \sum_{k=-\infty}^{\infty} h_0(k)\; x(2n-k) \tag{2}$$

$$H_1(n) = \sum_{k=-\infty}^{\infty} h_1(k)\; x(2n-k) \tag{3}$$

where L_1 and H_1 stand for the low-frequency approximation coefficients and the high-frequency detail coefficients of level 1, resp. To obtain L_2 and H_2, we in this way decompose the approximation coefficients L_1, etc. With the increasing decomposition level, the number of the coefficients decreases while the frequency resolution increases and moves to lower frequencies.

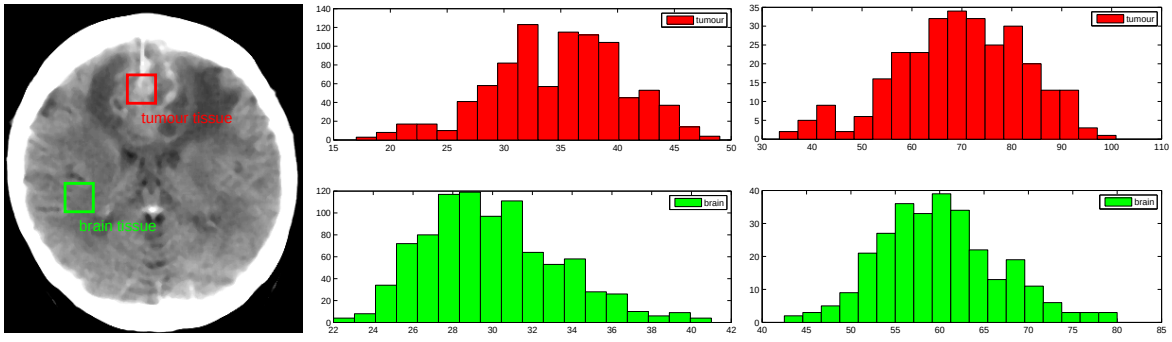

(a) Selected image regions (b) Regions histograms (c) Histograms of LL_1

Figure 2: Selected brain and tumour regions **(a)** and their histogram in space **(b)** and in the wavelet domain for LL_1 subband **(c)**

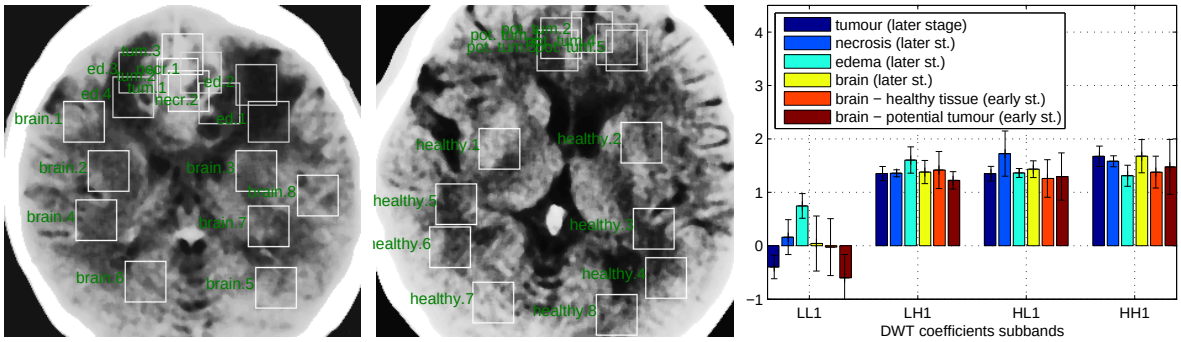

(a) Patient 1, later stage (b) Patient 1, early stage (c) Skewness of the DWT coefficients

Figure 3: The mean and the standard deviation value of the skewness for selected subbands of the absolute DWT coefficients **(c)** from the selected CT image regions in the later **(a)** and in the early tumour stage **(b)**

Thanks to its separability, the 1-Dimensional (1D) DWT described above can be easily applied to 2D images. We thus compute 1D DWT of the image row-wise, and then process the output column-wise. As a result, we obtain four instead of two coefficients subbands for each decomposition level commonly abbreviated as LL, LH, HL and HH.

In this paper, we compute the 2D DWT to level 1 and use the LeGall 5/3 biorthogonal filters [1]. The features are extracted using a rectangular sliding window of the size 28×28. To increase the number of samples, two adjacent image slices are also included into the computation, and thus the window size is 28×28×3 (see Fig. 1a for illustration). We do not use more slices than three because of relatively high slice thickness (3 mm) which implies that individual slices differ a lot in terms of their image content.

We finally selected the following features by analyzing their impact on the segmentation results and cluster compactness, suitable statistical characteristics allowing to distinguish between different ROI's and recognize similar ROI's (see Fig. 2 and 3), and also by using the leave-one-out method [8].

1. The skewness in the space domain
2. The skewness in the wavelet domain, namely the skewness of the absolute values of LL, LH, HL and HH coefficients of level 1
3. The mean of the LL coefficients of level 1

We examined a range of features including the mean and the standard deviation both in the space domain and the wavelet domain. However, only the mean of the LL_1 coefficients produced acceptable results.

3 Region Classification Using Neural Networks

Since 1980's, artificial Neural Networks (NN) [9, 10] have been successfully used in a wide range of signal and image processing applications such as signal prediction, noise reduction, and pattern classification. In this paper, we apply a self-organizing NN for extracted features classification.

Within the segmentation process, each image region confined by a rectangular window is represented by a feature vector of length R. These vectors computed for Q selected regions are organized in the pattern matrix $\mathbf{P}_{R,Q}$ and form clusters in the R-dimensional space. The Q pattern vectors in $\mathbf{P}$ are fed into the input NN layer, while the number C of the output

```
 %% Image Regions classification
P = normc(P); % normalize feature vectors
net = newc(minmax(P),C,alpha); % Create competitive NN layer
net.trainParam.epochs = no_epochs; % set no.  training epochs
net = train(net,C); % train NN
W = net.IW{1,1}; % 1-layer NN weights
A = sim(net,P); % simulate NN
Ac = vec2ind(A); % obtain class numbers
```

Figure 4: Algorithm for classification of the pattern matrix $\mathbf{P}$ into C classes and optimization of the weights $\mathbf{W}$ using the Matlab Neural Network Toolbox [5]

layer elements represents the desired number of segmentation classes. In each epoch of the network training process, the network weights $\mathbf{W}_{C,R}$ are recalculated by minimizing the distances between each input pattern vector and the corresponding weights of the winning neuron characterized by its coefficients closest to the current pattern [10]. In case that the process is successfully completed, the network weights belonging to separate output elements represent typical class individuals. Fig. 4 presents Matlab code for the training and simulation procedure.

In this paper, the region segmentation process comprises of training the NN on all image regions extracted by a rectangular sliding window with half overlap, and subsequent exploitation of the trained network for region classification. The algorithm comprises of the following successive steps

1. Feature vectors computation to create the feature matrix $\mathbf{P}$ using the sliding window
2. Initialization of the learning process coefficients and the network weights matrix $\mathbf{W}$
3. Iterative application of the competitive process and the Kohonen learning rule [10] for all feature vectors during the learning stage
4. NN simulation to assign class numbers to individual feature vectors
5. Evaluation of the regions classification results

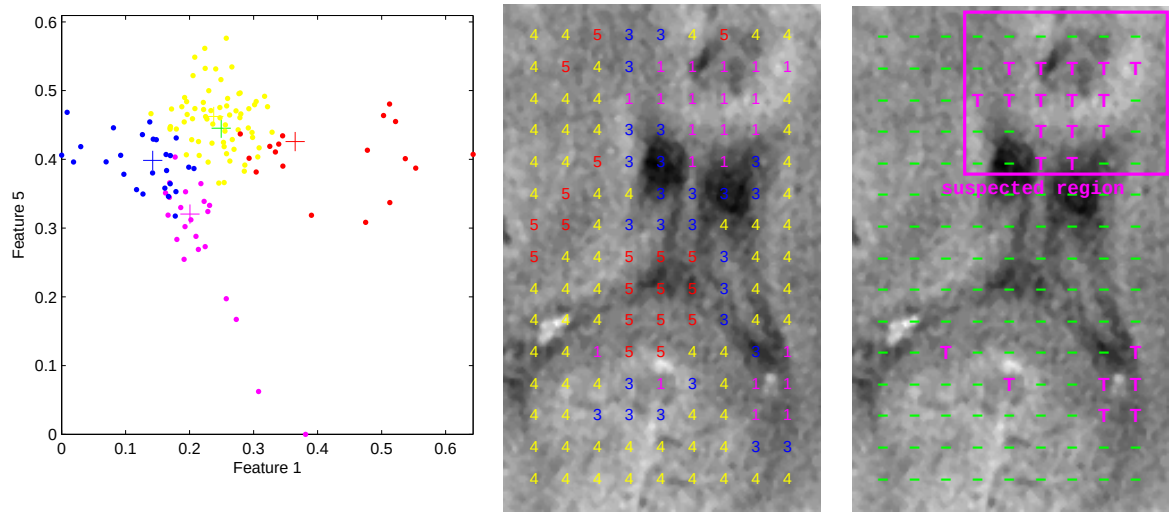

(a) Feature clusters (b) NN classification result (c) Tumour detection

Figure 5: Segmentation results for patient 1 presenting clusters for features 1 and 5 **(a)**, classification by the neural network **(b)**, and tumour detection **(c)** with the marked suspected region and regions classified as tumour

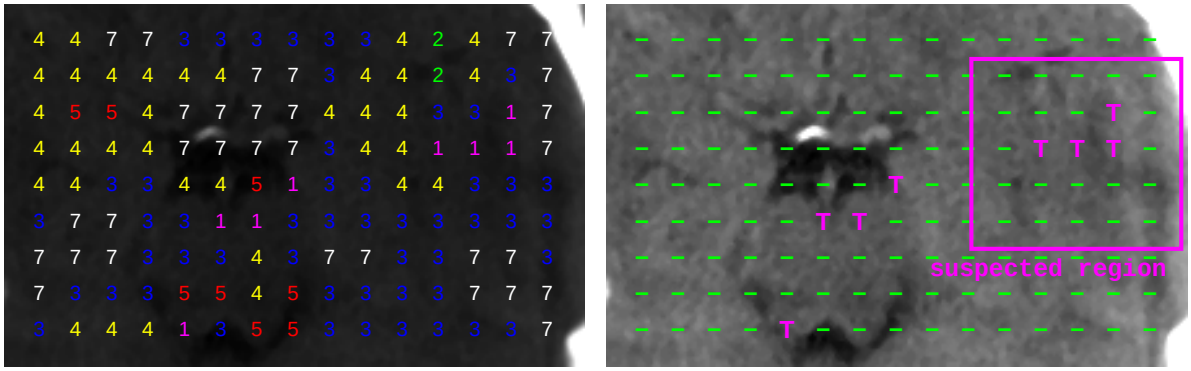

(a) NN classification result

(b) Tumour detection

Figure 6: Segmentation results for patient 2 displaying classification by the neural network **(a)**, and tumour detection **(b)** with the marked suspected region and regions classified as tumour

To evaluate the results of Q image segments classification into C classes, we exploit the *Cluster Segmentation Criterion* (CSC) [2]. This criterion is designed in the following manner. Each class $i = 1, 2, \ldots, C$ of N_i assigned segments is characterized by the mean Euclidian distance d_i of the column feature vectors $\mathbf{P}_{\bullet j_k}$ corresponding to the class members indices $\{j_k\}_{k=1}^{N_i}$ from the class center stated in the i-th row $\mathbf{W}_{i\bullet}$ of the weight matrix given by relation

$$d_i = \frac{1}{N_i} \sum_{k=1}^{N_i} \mathrm{dist}(\mathbf{P}_{\bullet j_k}, \mathbf{W}_{i\bullet}) = \frac{1}{N_i} \sum_{k=1}^{N_i} \sqrt{\sum_{r=1}^{R} (P_{r,j_k} - W_{i,r})^2} \tag{4}$$

The classification results can thus be characterized by the mean of intra-class distances related to the mean of the class-center distances representing $\binom{C}{2}$ combinations.

$$CSC = \frac{1}{C} \sum_{i=1}^{C} d_i \; / \; \frac{1}{\binom{C}{2}} \sum_{m=1}^{C-1} \sum_{n=m+1}^{C} \sqrt{\sum_{r=1}^{R} (W_{m,r} - W_{n,r})^2} \tag{5}$$

This criterion produces low values for compact and well separated clusters while closely spaced clusters with extensive dispersion result in high CSC values.

4 Results

Apart from evaluating clusters compactness using the CSC criterion, it is important for the algorithm setup to evaluate the *percentage of regions misclassified as tumour* by comparing the automated segmentation results with the correct image segmentation which is carried out manually exploiting the knowledge of tumour position from the images of later stages. Tab. 1 summarizes the segmentation results for two patients.

The CT image segmentation results are displayed in Fig. 5 and Fig. 6. The subimages on the right of both figures present the tumour diagnostics results. The pink rectangle marks the region, where we suspect the tumour to have already originated and pink letter 'T' labels regions classified as the tumour.

Table 1: The Overall Segmentation Results for Patient 1 and Patient 2

Patient Number	*Cut Size*	*Percentage of Regions Misclassified as Tumour*	*CSC Criterion*
1	224×140	31.8 %	0.47
2	140×224	57.1 %	0.33

Images of both patients are segmented by feature classification into five classes. In case of patient 1, the resulting number of classes is four. In case of patient 2, the resulting number of classes is five while the number 7 in Fig. 6 signifies the regions excluded from classification as outliers owing to the content of the bone tissue.

5 Conclusions

As demonstrated above, the proposed method of CT image content recognition gives good results which is quite promising for the future work on automated glioma diagnostics support. Further effort should be aimed at improving the feature clusters quality by finding the best features combination and automating the evaluation of the neural network classification output. The improved method should then be tested for more image datasets and the results should be further consulted with the neurologist.

ACKNOWLEDGEMENTS

We would like to thank Dr. O. Vyšata for his help and valuable advice.

This paper has been funded by the research grant of the Faculty of Chemical Engineering of the Institute of Chemical Technology, Prague no. MSM 6046137306 and VG 445089038.

References

[1] A. N. Akansu, R. A. Haddad. *Multiresolution Signal Decomposition: Transforms, Subbands and Wavelets*. Academic Press, San Diego, USA, 2001.

[2] A. Procházka, E. Hošťálková, A. Gavlasová. Wavelet Transform in Image Regions Classification. In *Proceedings of the 8th IMA Conference on Mathematics in Signal Processing*, pages 34–38, Cirencester, UK, 2008.

[3] D. B. Percival, A. T. Walden. *Wavelet Methods for Time Series Analysis*. Cambridge Series in Statistical and Probabilistic Mathematics. Cambridge University Press, New York, USA, 2006.

[4] I. Pitas, A. N. Venetsanopoulos. *Nonlinear Digital Filters: Principles and Applications*. Kluwer Academic Publisher, 1990.

[5] G. Oppenheim J. M. Poggi M. Misiti, Y. Misiti. *Wavelet Toolbox*. The MathWorks, Inc., Natick, Massachusetts 01760, April 2001.

[6] M. Petrou, V. Kovalev. Statistical Differences in the Grey Level Statistics of T1 and T2 MRI Data of Glioma Patients. *International Journal of Scientific Research*, 15:119–123, 2005.

[7] M. Petrou, V. Kovalev, J. R. Reichenbach. Three-Dimensional Nonlinear Invisible Boundary Detection. *IEEE Transaction on Image Processing*, 15:119–123, 2006.

[8] M. S. Nixon, A. S. Aguado. *Feature Extraction & Image Processing*. Academic Press, Elsevier, 2nd edition, 2008.

[9] S. Haykin. *Neural Networks, A Comprehensive Foundation*. Macmillan College Publishing Company, New York, 1994.

[10] T. Kohonen. *Self-organizing Maps*. Springer Verlag, third edition, 2001.

Zdeněk Měřínský, Eva Hošťálková, and Prof. Aleš Procházka
Institute of Chemical Technology, Prague
Department of Computing and Control Engineering
Technická 1905, 166 28 Prague 6
Phone.: +420-220 442 970, +420-220 444 198, Fax: +420-220 445 053
Zdenek.Merinsky@vscht.cz, Eva.Hostalkova@vscht.cz , A.Prochazka@ieee.org
http://dsp.vscht.cz